24th Australasian Fluid Mechanics Conference – AFMC2024
Canberra Australia
1-5 December 2024

Paper No: AFMC2024-17
DOI:10.5281/zenodo.14213370

Turbulence and Secondary Motion in Rectangular Channels: Implications for Upstream Fish Passage at Road Crossings

Hui Ling Wong [1*] and Hubert Chanson [1]

[1] The University of Queensland, School of Civil Engineering, Brisbane QLD 4072, Australia
* Email: huiling.wong@uqconnect.edu.au

Abstract

A culvert is a covered channel designed to pass water through an embankment. The adverse ecological impacts of road crossings on upstream fish passage have driven the development of new design guidelines with a focus on small-bodied native fish species and juveniles of larger fish. Recent studies recommended the usage of low velocity zones (LVZ) in the culvert for upstream fish passage. To date, there is a limited knowledge on the hydrodynamics in the LVZ, particularly the turbulence characteristics, despite its relevance to fish kinematics. New research was carried out to study the turbulence and secondary motion in low velocity zone in a rectangular culvert. Detailed turbulence measurements were undertaken in a near full-scale box culvert barrel. Velocity and Reynolds stress measurements showed some strong secondary motion of Prandtl's second kind. The turbulent characteristics, including burst events and secondary currents, were carefully detailed, presenting a novel insight into the turbulence of fish's preferential swimming zone.

1. Introduction

A culvert is a narrow channel designed to carry water through an embankment (Henderson, 1966) (Fig. 1A). The large velocities in the culvert barrel prevent the upstream passage of fish with weak swimming abilities, particularly for small-bodied fish and juveniles of larger fish, leading to waterways fragmentation and isolation of the fish populations (Rolls et al., 2013). In the Greater Brisbane region, 44% of the 50 native freshwater fish species require unhindered access between the freshwater and the estuary to complete their life cycle and species distribution, particularly small-bodied fishes and the juveniles of the larger fish (Moore et al., 2018). This report listed 13629 potential barriers in the Greater Brisbane area alone. Some current initiatives include roughness manipulations and baffles installation in the culvert, although these initiatives reduce the hydraulic efficiency and discharge capacity of the structure during large floods. Common appurtenances such as baffles cause a massive reduction in the discharge capacity (Leng & Chanson, 2020b), resulting in a higher cost of culvert design and construction.

The broad literature acknowledges that fish prefer to swim upstream next to the culvert barrel sidewall, irrespective of the species (Katopodis & Gervais, 2016; Cabonce et al., 2019; Chanson & Leng, 2021; Miles et al., 2021). These regions have lower velocities compared to the mean flow velocity, and the fish pro-actively utilise these low velocity zones (LVZ) (Leng et al., 2019; Sailema et al., 2020; Chanson & Leng, 2021). While some studies attempted to characterise, manipulate and size the geometric dimensions of these LVZs in standard box culverts through channel widening (Leng et al., 2019; Leng & Chanson, 2020a), there are limited information on the turbulence characteristics of LVZ.

In a box culvert barrel, the strongest turbulence is generated in the corner regions with their effects seen in most parts of the channel (Prandtl, 1952). Secondary currents develop due to the hydrodynamic singularities generated by the corners and are associated with large turbulent Reynolds stresses next to the singularities. In turbulent flow, the presence of eddies of different timescale and length scale will also interfere with the fish locomotion. The moment produced by the vortex favours fish to overturn and lose stability, especially if the size of the vortex and the fish body length are

similar (Lupandin, 2005). All in all, the manifestation of these complicated hydrodynamic motions interacts with the kinematics and mechanics of fishes, presenting a non-trivial aspect to scrutinise.

This study aims to characterise the turbulence in the fish's preferential swimming zone, i.e. LVZ, of a rectangular culvert barrel. To date, the physical modelling was undertaken with a focus on secondary currents and turbulent flow field for a less-than-design discharge condition.

(A)   (B)

Figure 1, Culvert channel. (A) Prototype culvert in Indooroopilly, Australia during a large flood in February 2024. (B) Experimental facility at the University of Queensland with Prandtl-Pitot tube in operation (yellow arrow) – Flow direction from left to right in both photographs.

2. Methodology, Facility and Instrumentation

The physical experiments were conducted in a 15 m long 0.5 m wide horizontal rectangular channel, acting a 1:6.1 scale model of a barrel cell of the prototype structure, as seen in Figure 1A. The channel invert was smooth and horizontal. The water was supplied by a constant head reticulation system feeding a 2.0 m long, 1.25 m wide intake basin, equipped with baffles, flow straighteners and three-dimensional convergent section leading to the 0.5 m wide flume. The flume ended with a free overfall at the downstream end.

The flow rate was recorded using a Venturi meter placed on the supply pipeline. The centreline water depths were recorded with a pointer gauge, with an accuracy of ±0.5 mm. The water velocities were measured with a Dwyer® 166 Series Prandtl-Pitot tube and a Nortek™ Vectrino+ acoustic Doppler velocimeter (ADV) equipped with a side-looking head. The Prandtl-Pitot tube consisted of a Ø3.3 mm stainless steel tube seen in Figure 1B. The ADV unit was sampled at 200 Hz for 180 s at each location. All ADV signal data were post-processed to remove erroneous data and spikes. Data with an average correlation of less than 60% and an average SNR less than 5 dB were removed, and the signal was "despiked" using a phase-space thresholding technique (Goring and Nikora 2002; Wahl 2003).

Visual and free-surface observations were carried out for flow rates 0.029 $m^3/s < Q < 0.100$ m^3/s. Detailed velocity measurements were performed for $Q = 0.0556$ m^3/s at a longitudinal distance $x = 8$ m from the start of the channel (Table 1).

Bed slope, θ_b (°)	**Width, B (m)**	**Discharge, Q (m^3/s)**	**Depth, d (m)**	***Re* x=8m**	***Fr* x=8m**	***B*/*d* x=8m**	**Comment**
0	0.50	0.0290	0.099	1.7 E+05	0.59	5.05	Smooth Channel
		0.0556	0.144	2.8 E+05	0.65	3.47	
		0.1000	0.207	4.3 E+05	0.68	2.42	

Table 1. Flow and boundary conditions (Bed slope, Reynolds number and aspect ratio) for all experiments involved in the flow investigations.

3. Results

3.1 Free surface and Longitudinal Velocity

For all flow conditions, the free-surface flow was subcritical in the channel. The water depth was greater than the critical depth and the Froude number was less than unity. The Froude number is the ratio of the fluid inertial to the gravitational acceleration: $Fr = V/(g \times d)^{1/2}$ for a rectangular channel. The longitudinal free surface profiles were categorised as a H2 profile (Henderson, 1966; Chanson, 2004). The free surface data were analysed and yielded a Darcy-Weisbach friction factor from 0.0264 to 0.0216, with increasing Reynolds number. The Darcy-Weisbach friction factor is a dimensionless boundary shear stress.

The bulk of the flow corresponded to large time-averaged longitudinal velocities, with maximum velocity V_{max}/V_{mean} of 1.11 for Q = 0.0556 m^3/s and 0.100 m^3/s, where the bulk velocity $V_{mean} = Q/A$ and A is the flow cross-section area. The formation of two large velocity cells and a slight asymmetrical flow condition in the cross-section were observed from the time-averaged longitudinal velocity data (Fig. 2). The slight asymmetry could be due to the inlet flow condition, reflecting a real fluid flow that could be observed in a real full-scale culvert site. As the friction along the boundaries induced a momentum transfer from the high-velocity regions, the longitudinal velocity was reduced in the vicinity of the invert and sidewalls, and the velocity was zero at the boundary because of no-slip condition. Regions of low velocities, i.e. LVZs, were seen in the bottom corners and next to the sidewalls of the channel (Fig. 2).

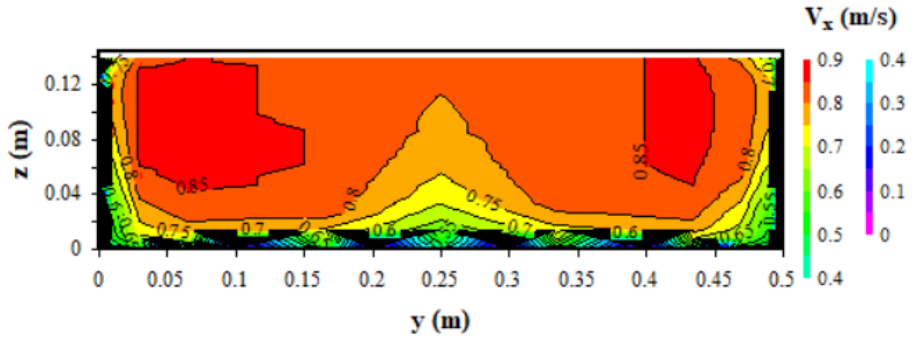

Figure 2. Contour plot of the time-averaged longitudinal velocity, $\overline{V_x}$ for Q=0.0556 m^3/s.

3.2 Secondary Currents

In a rectangular channel, the bottom corners played a key role for the secondary currents because a transverse flow was directed towards the corner as a direct result of turbulent shear stress gradients normal to the edge bisector (Prandtl, 1952; Gessner, 1973). The secondary current contour maps are shown in Figure 3 for Q = 0.0556 m^3/s. The magnitudes of secondary currents at the channel centreline were near zero. On each side of the channel centreline, the surface currents circulated towards the wall from the centreline, forming two vortical cells typical of Prandtl's second kind. The flow motion of a Prandtl's second kind refers to the presence of secondary-current motion in a straight channel, typically in a turbulent flow (Prandtl, 1952). The present data indicated some secondary current magnitudes, i.e. $(\overline{V_y}^2+\overline{V_z}^2)^{1/2}$, with a median value of 0.041 m/s and 90% percentile of 0.063 m/s, corresponding respectively to 4.7 % and 7.3% of the maximum velocity V_{max} for Q = 0.0556 m^3/s. A strong horizontal transverse flow, i.e., $|\overline{V_y}| > 0$, occurred near the free surface, as previously reported (Nezu and Rodi, 1985). A downward flow motion $\overline{V_z} < 0$ was observed next to both sidewalls, which could also be one of the key parameters in facilitating upstream fish passage near the sidewall.

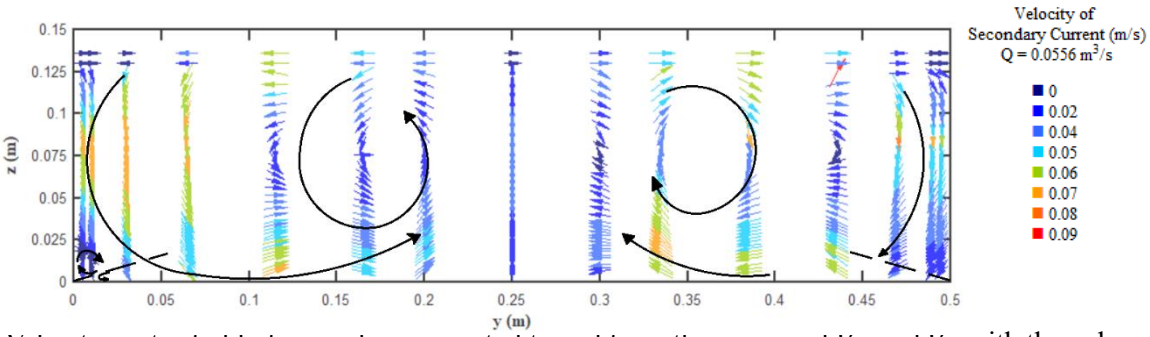

Figure 3. Velocity vector field of secondary current obtained from the measured V_y and V_z, with the colour codes as the magnitude of the secondary current and the separation line dividing the vortical cells in the corners for Q = 0.0556 m^3/s.

3.3 Turbulent Bursting

Burst events are random events in the time series which its intensity can increase by orders of magnitude locally (Narasimha et al., 2007; Hack & Schmidt, 2021). The consideration of burst events is relevant to fish passage as the amplitude of the burst, accompanied by long burst duration, could pose difficulties for fish to navigate. For the burst analysis in the context of fish passage, the amplitude, magnitude and burst duration of the turbulent flux were examined following Narasimha et al. (2007) and Trevethan and Chanson (2010). Typical contour plots are shown in Figures 4 and 5. The definition of the dimensionless amplitude, A_b of the burst event is defined as:

$$A_b = \frac{1}{\bar{q}_b} \int_{\tau} (q_b - \bar{q}_b) \frac{dt}{\tau_b} \quad (1)$$

where q_b is the instantaneous turbulent flux, i.e. $v_x \times v_x$, $v_x \times v_y$, $v_x \times v_z$, $v_y \times v_y$, $v_y \times v_z$ and $v_z \times v_z$,, $\bar{q}_b$ is the mean value of the turbulent flux, q_b, τ_b is the burst duration between the two consecutive mean intersection of the turbulent flux of a burst event, and dt is the time duration between two instantaneous turbulent fluxes, which is the inverse of the sampling frequency, f (200 Hz). The dimensionless amplitude expresses the ratio between the averaged flux amplitude during the event to the long-term mean flux of the entire data section. The median burst duration, amplitude and magnitude of the burst events for Q = 0.0556 m^3/s are presented in the form of contour plot, with typical plots shown in Figures 4 to 5. Overall, the contour mapping of the burst event showed burst events with larger amplitude and longer burst duration located near the sidewalls and the channel invert. Depending on the component of the turbulent flux, the distribution of burst event characteristics was not always symmetrical about the channel centreline. The amplitude of the normal turbulent fluxes, i.e., $v_x \times v_x$, $v_y \times v_y$ and $v_y \times v_y$ are relatively small, accompanied with a shorter burst duration compared to the tangential turbulent fluxes. By comparing both corners, the median burst duration and amplitude for $v_x \times v_x$, $v_y \times v_y$ and $v_y \times v_z$ are rather consistent and in the same order of magnitude. By comparing both the normal and tangential turbulent fluxes, the normal turbulent fluxes yield a higher total number of turbulent burst events. In the corners, the tangential turbulent fluxes, $v_x \times v_y$ and $v_x \times v_z$ were observed to have a larger median burst amplitude, i.e., $|A_b| > 20$, accompanied with a longer burst duration. As the distance from the channel invert increases, $|A_b|$ also decreases as shown in Table 2, with z = 0.0058 m and $z = z_{max}$ in the right corner as comparison.

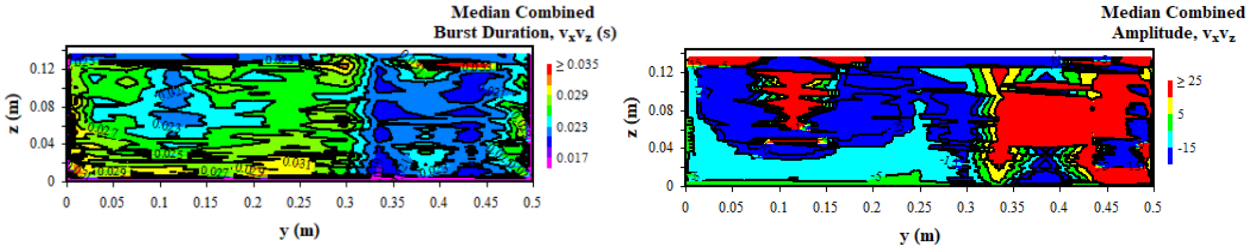

Figure 4. Turbulent median burst duration and amplitude for turbulent flux $v_x \times v_z$ of Q = 0.0556 m^3/s.

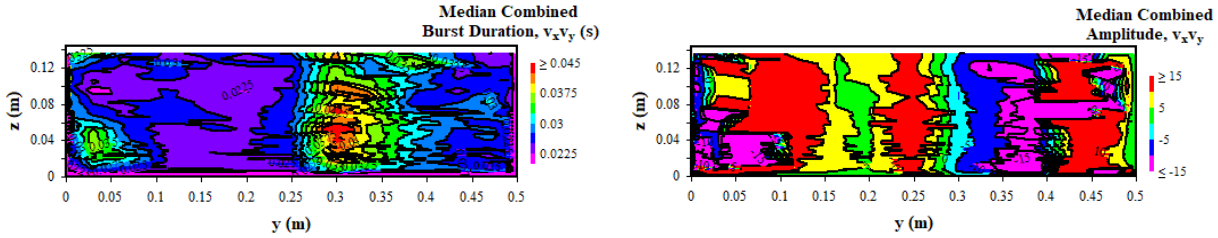

Figure 5. Turbulent median burst duration and amplitude for turbulent flux $v_x \times v_y$ of Q = 0.0556 m^3/s.

Turbulent Flux (m^2/s^2)	y (m)	z (m)	Median Burst Duration (s)	Median Burst Amplitude	Total No. of Events	No. of Burst with Sub-Event	Average Number of Sub-Events Per Burst Event
$v_x \times v_x$	0.005 (right corner)	0.0058	0.0148	1.529	1430	210	2.062
$v_x \times v_y$			0.0232	-99.628	505	191	2.162
$v_x \times v_z$			0.0296	-7.222	335	174	2.069
$v_x \times v_x$	0.495 (left corner)	0.0058	0.0156	1.405	1749	182	2.082
$v_x \times v_y$			0.0242	17.600	867	246	2.163
$v_x \times v_z$			0.0233	54.767	590	152	2.046
$v_x \times v_x$	0.25 (centreline)	0.1358 (z_{max})	0.0148	1.462	1609	225	2.089
$v_x \times v_y$			0.0282	13.690	702	326	2.294
$v_x \times v_z$			0.0211	-76.011	582	240	2.108
$v_x \times v_x$	0.005 (right corner)	0.1178 (z_{max})	0.0156	1.462	1470	227	2.040
$v_x \times v_y$			0.0280	-11.685	440	216	2.106
$v_x \times v_z$			0.0284	-7.971	359	148	2.061

Table 2. Burst characteristics of $v_x \times v_x$, $v_x \times v_y$, and $v_x \times v_z$ in the bottom corners – Comparison with elevation of maximum velocities, z_{max} near the sidewall and the centreline.

4. Discussion

The flow field in rectangular channels is traditionally divided into several layers, i.e., the viscous sublayer ($zu_*/\mu \leq 5$), buffer layer ($5 < zu_*/\mu < 30$), turbulent wall shear layer ($zu_*/\mu \geq 30$, $z/d < 0.2$), and turbulent outer layer ($0.2 \leq z/d \leq 1$) (Chanson, 2014; Dey, 2014), where z is the vertical distance from the channel invert, μ is the kinematic viscosity and u_* is the shear velocity. A typical flow field division is shown in Figure 6 with Q = 0.0556 m^3/s, d = 0.144 m and compared to the dimension of a typical small-bodied fish (Australian Smelt). The viscous sublayer and buffer layer were very thin compared to the dimension of the fish. The fish would swim in the LVZ, i.e. the turbulent wall shear layer, where the Reynolds shear stress is predominant and viscous shear stress is negligible. This wall shear layer is also the layer dominated by turbulent bursting. The occurrence of turbulent burst events is directly relevant to fish passage as the amplitude of the burst, accompanied by long burst duration in low velocity zones, could adversely impact the fish movements. In this study, the burst duration and amplitude were indeed found to be higher near the sidewall and the corners, with some dimensionless amplitude exceeding 10. An amplitude of 10 means that the averaged flux amplitude during the event is 10 times larger than the long-term mean flux of the entire data section. Such a large burst amplitude could potentially affect fish passage due to a sudden spike of turbulent stress.

A few studies showed that some fish species can sustain very high turbulent stresses, e.g. Iberian barbel with minimum total length of 150 mm could occupy areas with Reynolds stresses up to 60 Pa (Silva et al., 2011), while Hybrid Bass, Rainbow Trout and Atlantic salmon can be exposed to Reynolds shear stresses higher than 50 Pa without significant mortality, even when exposed for more than 48 hours (Odeh et al., 2002). There is still a lack of data on the threshold of Reynolds stresses that small-bodied fishes can withstand. As the Reynolds stresses and turbulent burst events are non-negligible in the LVZ, it would be most relevant to consider the Reynolds stresses that each fish species can withstand comfortably, including the extreme turbulent fluxes and its burst duration.

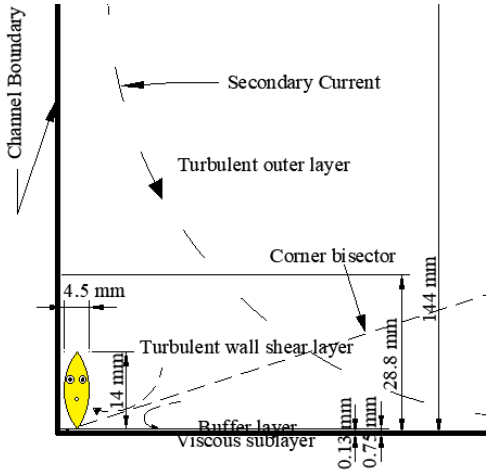

Figure 6. Turbulent flow field with secondary current in a box culvert corner, with a typical body size of Australian Smelt and flow characteristics of Q = 0.0556 m^3/s, d = 0.144 m

5. Conclusion

New research has been carried out with the focus on the hydrodynamic characterisation of low velocity zones in rectangular channels, because these low velocity regions are the preferential swimming zones in standard box culvert barrel. Some detailed physical modelling was carried out in a near-full-scale box culvert barrel, 0.5 m wide and 15 m long. Velocity and turbulence measurements were performed for a range of flow conditions, corresponding to less-than-design flood events, during which fish may attempt to traverse upstream the structure. A sizable low velocity zone was documented through physical modelling, with a downward secondary current flow motion $\overline{V_z} < 0$ observed next to both sidewalls.

Three-dimensional velocity measurements showed some strong secondary motion of Prandtl's second kind. For this range of less-than-design flow condition, the LVZ lied within the turbulent wall shear layer, which consisted of intense turbulent burst events with large amplitude and long burst duration. Interestingly, the sidewall and corner regions with the higher Reynolds stress and burst events also constitute a lower Eulerian timescale and advection length scale, thus providing a conducive space for fish to navigate. The outcome of the physical modelling provided a fascinating insight into the hydrodynamics of the fish's preferential swimming zone.

Acknowledgments

The authors acknowledge the technical assistance for Jason Van Der Gevel and Stewart Matthews (The University of Queensland). They also acknowledge the financial support of Apiary Financial (Grantor RE333704). Hui Ling Wong acknowledges the financial support of the Research Training Program (RTP), funded by the Commonwealth Government of Australia and the University of Queensland.

References

Cabonce, J., Fernando, R., Wang, H., & Chanson, H. (2019). Using small triangular baffles to facilitate upstream fish passage in standard box culverts. *Environmental Fluid Mechanics*, 19(1), 157–179. DOI: 10.1007/s10652-018-9604-x

Chanson, H. (2004). *The Hydraulics of Open Channel Flow: An Introduction*. Butterworth-Heinemann, 2nd edition, Oxford, UK, 630 pages.

Chanson, H. (2014). *Applied Hydrodynamics: An Introduction*. CRC Press, Taylor & Francis Group, Leiden, The Netherlands, 448 pages & 21 video movies

Chanson, H., & Leng, X. (2021). *Fish Swimming in Turbulent Waters: Hydraulic Engineering Guidelines to assist Upstream Passage of Small-Bodied Fish Species in Standard Box Culverts.*

CRC Press, Taylor and Francis Group, Leiden, The Netherlands. 202 pages and 19 video movies. DOI: 10.1201/9781003029694

Dey, S. (2014) *Fluvial Hydrodynamics: Hydrodynamic and Sediment Transport Phenomenon*. Springer Berlin, Heidelberg. 687 pages. DOI: 10.1007/978-3-642-19062-9

Gessner, F.B. (1973) The Origin of Secondary Flow in Turbulent Flow along a Corner. *Journal of Fluid Mechanics*, Vol. 58, Part 1, 1-25.

Goring, D.G., and Nikora, V.I. (2002). Despiking Acoustic Doppler Velocimeter Data. *Jl of Hyd. Engrg.*, ASCE, Vol. 128, No. 1, pp. 117-126. Discussion: Vol. 129, No. 6, pp. 484 - 489.

Hack, M., & Schmidt, O. (2021). Extreme events in wall turbulence. *Journal of Fluid Mechanics*, 907, A9. DOI: 10.1017/jfm.2020.798

Henderson, F.M. (1966). *Open Channel Flow*. MacMillan Company, New York, USA.

Katopodis, C., & Gervais, R. (2016). Fish Swimming Performance Database and Analyses. *DFO CSAS Research Document No. 2016/002*, Canadian Science Advisory Secretariat, Fisheries and Oceans Canada, Ottawa, Canada, 550 pages.

Leng, X., Chanson, H., Gordos, M., & Riches, M. (2019). Developing Cost-Effective Design Guidelines for Fish-Friendly Box Culverts, with a Focus on Small Fish. *Environmental Management*, 63(6), 747–758. DOI: 10.1007/s00267-019-01167-6

Leng, X., & Chanson, H. (2020a). Hybrid modelling of low velocity zones in box culverts to assist fish passage: Why simple is better! *River Research and Applications*, 36(9), Review Paper 1765–1777. DOI: 10.1002/rra.3710

Leng, X., & Chanson, H. (2020b). Full-height sidewall baffles in box culvert to assist upstream fish passage: Physical modelling. *Proceedings of the 8th IAHR International Symposium on Hydraulic Structur*es ISHS 2020, 12-15 May 2020, Santiago, Chile, 10 pages. DOI: 10.14264/uql.2020.581

Lupandin A.I. (2005). Effect of flow turbulence on swimming speed of fish. *Biology Bulletin Russ Acad Sci.*, 32(5), 461–466. DOI: 10.1007/s10525-005-0125-z

Miles, J., Vowles, A. S., & Kemp, P. S. (2021). The response of common minnows, Phoxinus phoxinus, to visual cues under flowing and static water conditions. *Animal Behaviour*, 179, 289–296. DOI: 10.1016/j.anbehav.2021.07.004

Moore, M., Mccann, J., & Power, T. (2018). Greater Brisbane Fish Barrier Prioritisation. Report for Re-Connecting Aquatic Habitats Across the Greater Brisbane Urban Area

Narasimha, R., Kumar, S.R., Prabhu, A., and Kailas, S.V. (2007). Turbulent Flux Events in a Nearly Neutral Atmospheric Boundary Layer. *Phil. Trans. Royal Soc*., Series A, Vol. 365, pp. 841-858.

Nezu, I., & Rodi, W. (1985). Experimental Study on Secondary Currents in Open Channel Flow. *Proceedings 21st IAHR Biennial Congress*, Melbourne, Australia, pp. 114-119.

Nezu, I & Nakagawa, H. (1993) *Turbulence in Open Channel Flows*. Routledge, London. DOI:10.1201/9780203734902

Odeh, M., Noreika, J.F., Haro, A., Maynard, A., & Castro-Santos, T. (2002) Evaluation of the Effects of Turbulence on the Behavior of Migratory Fish. *Report to the Bonneville Power Administration*, Contract no. 00000022, Project no. 200005700 (BPA Report DOE/BP-00000022-1).

Prandtl, L. (1952) *Essentials of Fluid Dynamics with Applications to Hydraulics, Aeronautics, Meteorology and Other Subjects*. Blackie & Son, London, UK, 452 pages.

Rolls, R. J., Ellison, T., Faggotter, S., & Roberts, D. T. (2013). Consequences of connectivity alteration on riverine fish assemblages: Potential opportunities to overcome constraints in applying conventional monitoring designs. *Aquatic Conservation: Marine and Freshwater Ecosystems*, 23(4), 624–640. DOI: 10.1002/aqc.2330

Sailema, C., Freire, R., Chanson, H., & Zhang, G. (2020). Modelling small ventilated corner baffles for box culvert barrel. *Environmental Fluid Mechanics*, 20(2), 433–457. DOI: 10.1007/s10652-019-09680-2

Silva, A.T, Santos, J.M., Ferreira M.T., Pinheiro, A.N., & Katopodis, C. (2011) Effects of water velocity and turbulence on the behaviour of Iberian barbel (Luciobarbus bocagei, Steindachner 1864) in an experimental pool-type fishway. *River Research and Applications*. 44. 360-373.

Trevethan, M., & Chanson, H. (2010). Turbulence and turbulent flux events in a small estuary. *Environ Fluid Mech* 10, 345–368. DOI: 10.1007/s10652-009-9134-7

Wahl, T.L. (2003). Despiking Acoustic Doppler Velocimeter Data. Discussion. *Jl of Hyd. Engrg.*, ASCE, Vol. 129, No. 6, pp. 484-487.